

# Organic & Biomolecular Chemistry

Accepted Manuscript



This article can be cited before page numbers have been issued, to do this please use: X. Yu, X. Hong and W. Chen, *Org. Biomol. Chem.*, 2019, DOI: 10.1039/C8OB03036G.



This is an Accepted Manuscript, which has been through the Royal Society of Chemistry peer review process and has been accepted for publication.

Accepted Manuscripts are published online shortly after acceptance, before technical editing, formatting and proof reading. Using this free service, authors can make their results available to the community, in citable form, before we publish the edited article. We will replace this Accepted Manuscript with the edited and formatted Advance Article as soon as it is available.

You can find more information about Accepted Manuscripts in the [author guidelines](#).

Please note that technical editing may introduce minor changes to the text and/or graphics, which may alter content. The journal's standard [Terms & Conditions](#) and the ethical guidelines, outlined in our [author and reviewer resource centre](#), still apply. In no event shall the Royal Society of Chemistry be held responsible for any errors or omissions in this Accepted Manuscript or any consequences arising from the use of any information it contains.

## Fluorinated bisbenzimidazoles: a new class of drug-like anion transporters with chloride-mediated, cell apoptosis-inducing activity

Received 00th January 20xx,  
Accepted 00th January 20xx

DOI: 10.1039/x0xx00000x

[www.rsc.org/](http://www.rsc.org/)

Xi-Hui Yu<sup>#</sup>, Xiao-Qiao Hong<sup>#</sup> and Wen-Hua Chen<sup>\*</sup>

Anion transporters have attracted substantial interest due to their ability to induce cell apoptosis by disrupting cellular anion homeostasis. In this paper we describe the synthesis, anion recognition, transmembrane anion transport and cell apoptosis-inducing activity of a series of fluorinated 1,3-bis(benzimidazol-2-yl)benzene derivatives. These compounds were synthesized from the condensation of 1,3-benzenedialdehyde or 5-fluoro-1,3-benzenedialdehyde with the corresponding 1,2-benzenediamines and fully characterized. They are able to form stable complexes with chloride anions, and exhibit potent liposomal and *in vitro* anionophoric activity. Their anion transport efficiency may be ameliorated by the total number of fluorine atoms, and the enhanced anionophoric activity was a likely consequence of the increased lipophilicity induced by fluorination. Most of these fluorinated bisbenzimidazoles exhibit potent cytotoxicity toward the selected cancer cells. Mechanistic investigations suggest that these compounds are able to trigger cell apoptosis probably by disrupting the homeostasis of chloride anions.

### 1. Introduction

It is known that cellular anion homeostasis is essential for cells to exert their biological function and imbalanced anion homeostasis may result in cell deaths. Among the anionic species in living systems, chloride anions are the most abundant ones in extracellular fluid and play a critical role in regulating cell death.<sup>1</sup> Therefore, it is believed that one compound that is able to disturb the homeostasis of chloride anions or modify the internal pH of cells, may be developed as a chemotherapeutic agent for the treatment of cancers.<sup>2,3</sup> During the past decades, this hypothesis has been attracting substantial interest in identifying transmembrane anion transporters, in particular for chloride anions.<sup>3-11</sup> These endeavours have been further driven forward by the findings that the transport properties of some anion transporters, for example, prodigiosin and its derivatives, are linked to their biological activity as anticancer agents.<sup>12-20</sup> As a consequence, diverse approaches have been adopted to optimize the anion transport and potential biological activity of anion transporters.

Fluorination represents a general strategy to ameliorate the transport activity and cytotoxicity of small-molecular anion transporters.<sup>3</sup> Because of the electron-withdrawing properties of fluorine atoms and the ability to increase the lipophilicity,<sup>21</sup> fluorination can enhance anion-binding affinity and/or membrane

partitioning, and as a consequence it is able to boost transport rates in a number of synthetic systems.<sup>22-25</sup> For example, Davis *et al* have reported that perfluorination of the acyl tail in monoacylglycerols affords synthetic anion transporters with improved chloride transport properties.<sup>22</sup> Gale *et al* have demonstrated that fluorination of a series of structurally simple urea and thiourea compounds leads to a significant increase in the transmembrane anion transport activity.<sup>23</sup> They have further reported that some *ortho*-phenylenediamine bis-ureas having fluorinated central phenyl ring and/or peripheral phenyl groups, are highly effective anion transporters and even outperform prodigiosin, the most active anion transporter known to date.<sup>24</sup> In addition, fluorination may also lead to an alteration in the mechanism of action of ion transport. For example, Gale *et al* have shown that calix[4]pyrrole acts as a CsCl symporter, whereas the octafluoro analogue functions as an anion exchanger.<sup>25</sup> On the other hand, fluorination is able to produce potent anion transporters by increasing the anion binding affinity and/or the lipophilicity of the receptors. For example, Gale *et al* have shown that fluorination of tripodal trisureas and trithioureas significantly improves the anion transport efficiency both in vesicular models and *in vitro*, with the best transporters depolarizing acidic compartments within GLC4 cells, reducing cell viability and inducing apoptosis in a range of human cancer cell lines, whilst the non-fluorinated analogues have a limited effect on cell viability.<sup>16</sup> They have further shown that even simple monoureas and thioureas containing fluorinated indoles display promising anticancer activity towards A375 melanoma cells.<sup>23</sup> Recently they have shown that fluorinated anion transporters, such as squaramides having trifluoromethylphenyl substituents, are able to trigger cell death *via* an apoptotic pathway and disturb the autophagy of cells.<sup>26</sup> These findings have spurred

Guangdong Provincial Key Laboratory of New Drug Screening, School of Pharmaceutical Sciences, Southern Medical University, Guangzhou 510515, P. R. China. E-mail: whchen@smu.edu.cn

<sup>#</sup> These authors contributed equally to this work.

<sup>†</sup> Electronic Supplementary Information (ESI) available: Structural characterization and experimental data for the anion recognition, anion transport and biological activity of each compound. See DOI: 10.1039/x0xx00000x

great efforts to systematically study the effect of fluorination on the anion transport and biological activity of anion transporters.

To respond to this as well as to develop small-molecule, drug-like anion transporters having both potent anion transport and biological activity, in previous studies we have reported that 1,3-bis(benzimidazol-2-yl)benzene (Bimbe **1**, Fig. 1) functions as an anion transporter and the activity may be significantly improved by adding electron-withdrawing substituents onto the benzimidazolyl subunits and/or the central phenyl moiety.<sup>27,28,29</sup> For example, <sup>5</sup>F<sub>2</sub>-Bimbe **3** (Fig. 1) having a fluorine atom at each terminal benzimidazolyl subunit exhibits *ca* 10-fold higher anionophoric activity than Bimbe **1**.<sup>28</sup>

Inspired by these findings, in this study we utilized fluorination as an alternative means to optimize the activity of Bimbe **1** with the aim to obtain insightful structure-activity correlations, and systematically studied the effect of fluorination on the transport and biological activity. Specifically, we designed and synthesized two series of fluorinated bis(benzimidazolyl) derivatives, that is, <sup>m1,m2,...Fn</sup>-Bimbe **2-6** based on Bimbe **1** and <sup>m1,m2,...Fn</sup>-FBimbe **8-13** based on 5-fluoro-1,3-bis(benzimidazol-2-yl)benzene (FBimbe, **7**) (Fig. 1). Here <sup>m1,m2,...Fn</sup>-Bimbe represents a Bimbe derivative having totally *n* fluorine atoms at the *m1,m2,...*-positions of the terminal benzimidazolyl subunits, whereas <sup>m1,m2,...Fn</sup>-FBimbe stands for an FBimbe derivative having totally *n* fluorine atoms at the *m1,m2,...*-positions of the terminal benzimidazolyl subunits. Most of these compounds have drug-like features required by the Lipinski's Rule of Five,<sup>30</sup> including molecular masses of smaller than 500, two hydrogen donor/acceptor groups and moderate lipophilicity. We carried out a systematic investigation into their anion recognition, anion transport, biological activity and the probable mechanism of biological action.

## 2. Results and discussion

### Chemistry

The new fluorinated derivatives **2** and **4-13** were synthesized from the one-step reaction of 1,3-benzenedialdehyde or 5-fluoro-1,3-benzenedialdehyde with the corresponding 1,2-benzenediamines (Scheme 1).<sup>27-29</sup> Bimbe **1** and <sup>5</sup>F<sub>2</sub>-Bimbe **3** have been previously reported by us and others.<sup>28,31</sup> 5-Fluoro-1,3-benzenedialdehyde was prepared from 1-fluoro-3,5-dimethyl-benzene in two steps according to reported protocols.<sup>32</sup> Compounds **2** and **4-13** were fully characterized on the basis of melting points (m.p.), ESI MS (LR and HR) and NMR (<sup>1</sup>H and <sup>13</sup>C) data (see experimental section and S1).

### Anion recognition

It is known that fluorination may enhance the activity of an anion transporter by increasing the hydrogen-bonding donor acidity and anion-binding affinity.<sup>22-25</sup> To evaluate how anion binding contributes to the transport efficiency of these fluorinated compounds, we studied their anion recognition properties toward chloride anions as tetra(*n*-butyl)ammonium salt (TBACl) by means of <sup>1</sup>H NMR titrations in acetonitrile. As shown in Fig. 2a and Fig. S48-S73, addition of TBACl led to significant downfield shifts of the benzimidazolyl NHs and the central aromatic H-2's, indicative of the hydrogen-bonding interactions with chloride anions. Only one set of

the benzimidazolyl NHs was observed, suggesting that both benzimidazolyl NHs are simultaneously involved in the interactions with chloride anions. These results suggest that chloride anions are bound to the core 1,3-bis(benzimidazol-2-yl)benzene moiety through the cooperative interactions with the benzimidazolyl NHs and the central aromatic H-2's, as reported in literature.<sup>29,31</sup>

Molar ratio assays indicate that the changes in the chemical shifts of the benzimidazolyl NHs or the central aromatic H-2's with the concentrations of each compound, follow a 1 : 1 binding mode with chloride anions (Fig. S48-S73). This 1 : 1 stoichiometry was further supported by means of ESI MS spectrometry. As shown in Fig. 2(b) and Fig. S74, these compounds are able to form stable 1 : 1 complexes with chloride anions. For example, in the negative ESI MS spectrum of <sup>5,6</sup>F<sub>4</sub>-FBimbe **12** mixed with TBACl (Fig. 2(b)), in addition to the ion peak at *m/z* = 399.66 ([<sup>5,6</sup>F<sub>4</sub>-FBimbe - H]<sup>-</sup>), a new ion peak at *m/z* = 435.59 was detected. This new ion peak is assignable to the complex of <sup>5,6</sup>F<sub>4</sub>-FBimbe **12** with chloride anions ([<sup>5,6</sup>F<sub>4</sub>-FBimbe + Cl]<sup>-</sup>). Nonlinear fitting analysis of the relationship between the chemical shift changes of the benzimidazolyl NHs (or the central aromatic H-2's) and the concentrations of each compound, according to a 1 : 1 binding model, affords the association constants (*K*<sub>a</sub>'s) with chloride anions (Table 1 and Fig. S48-S73). The association constants of compounds **1-13** with chloride anions were also measured in CH<sub>3</sub>CN/H<sub>2</sub>O (9/1, v/v) by means of spectrophotometric titrations. As shown in Fig. S75, addition of TBACl to compounds **1-13** led to a small change in the absorbance, which is indicative of the complex formation. The changes in the absorbance were analyzed against the concentrations of each compound, according to a 1 : 1 model, gave the association constants of compounds **1-13** with chloride anions (Table S1). The association constants obtained from both the <sup>1</sup>H NMR and spectrophotometric titrations demonstrate that these compounds show strong binding affinity toward chloride anions. Notably, compounds **2-6** exhibit very similar binding affinity toward chloride anions with compound **1**, whereas compounds **7-12** show higher affinity than the corresponding compounds **1-6**. This result suggests that fluorination on the central phenyl subunit may have more profound effect on the anion-binding affinity than on the benzimidazolyl subunits.

### Liposomal anion transport

*Ion transport efficiency.* To evaluate how fluorination ameliorates the ion transport efficiency of these compounds, we firstly measured the EC<sub>50</sub> value of each compound on liposomal models formed from egg-yolk *L*-α-phosphatidylcholine (EYPC), using a conventional pyranine assay (Fig. S76-S77 and Table S2).<sup>33</sup> Table 1 summaries the EC<sub>50</sub> and the Hill coefficient *n* values that were obtained from the Hill analysis of the relationship between the initial rate constants (*k*<sub>in</sub>'s) and the concentrations (mol%) of each compound.<sup>34</sup> As a consequence, these derivatives, in particular <sup>5,6</sup>F<sub>4</sub>-FBimbe **12** and <sup>4,5,6,7</sup>F<sub>8</sub>-FBimbe **13** exhibit high pH discharge activity. This result suggests that fluorination of Bimbe **1** may serve as a practical strategy to improve the ion transport activity. Calcein leakage assay (Fig. S78) clearly shows that these compounds do not disrupt the liposomal membranes.<sup>35</sup>

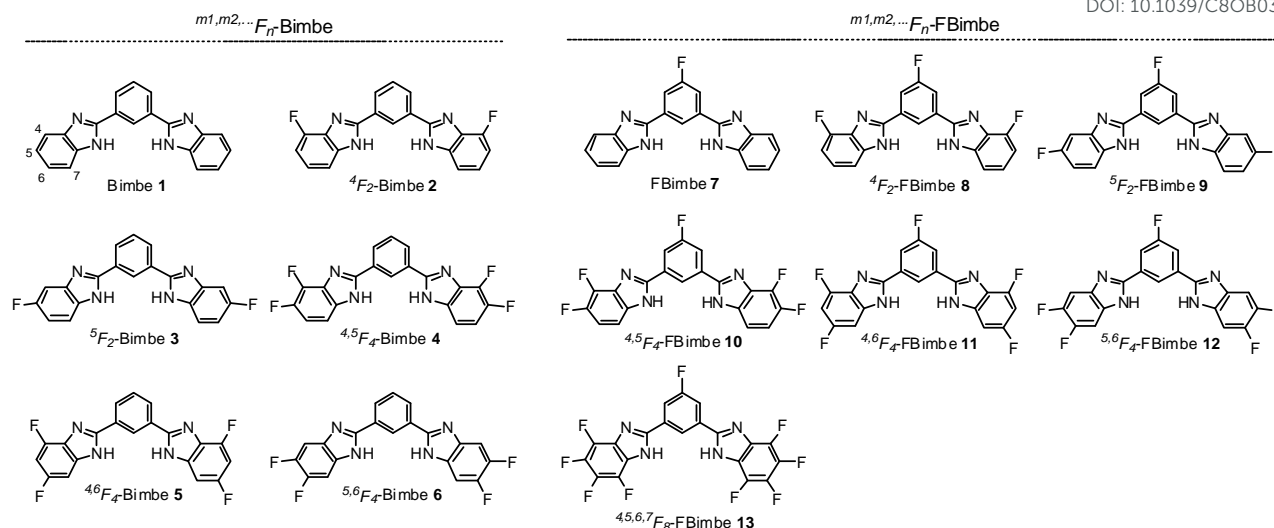
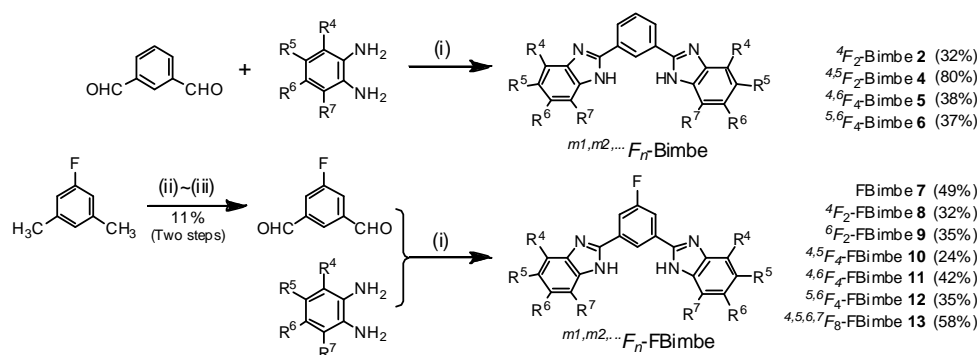


Fig. 1. Structures of Bimbe 1 and the fluorinated derivatives 2-13.



**Scheme 1.** Synthesis of fluorinated Bimbe derivatives 2 and 4-13. Reagents and conditions: (i) DMSO (or  $\text{CH}_3\text{CN}$ ), room temperature-reflux; (ii) NBS, AIBN,  $\text{CCl}_4$ , reflux, 8 h; (iii) concentrated  $\text{H}_2\text{SO}_4$ , 110 °C, 1 d. See Fig. 1 for the specific substituents  $\text{R}^4$ ,  $\text{R}^5$ ,  $\text{R}^6$  and  $\text{R}^7$ .

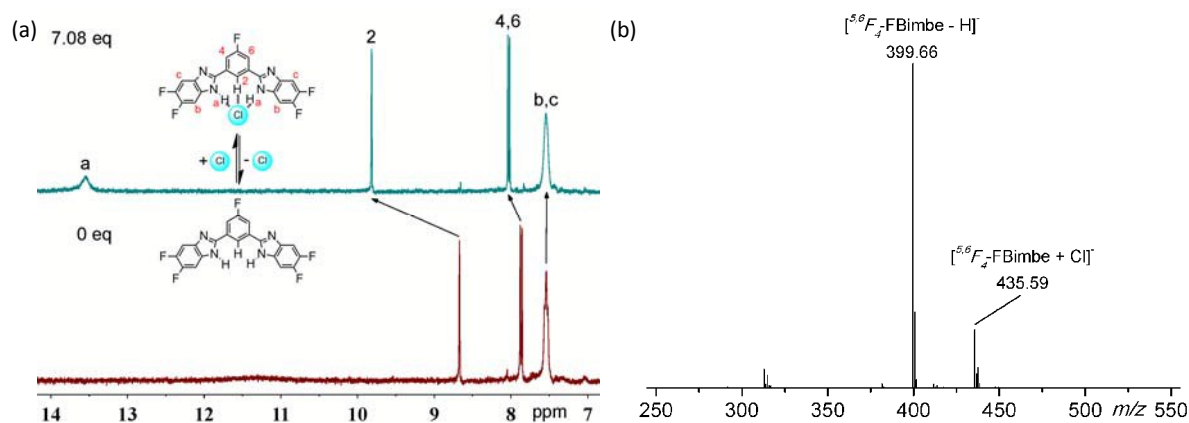


Fig. 2. (a)  $^1\text{H}$  NMR spectra (acetonitrile- $d_3$ , 400 MHz) of  $^5,6F_4$ -FBimbe 12 ( $1.0 \times 10^{-3}$  M) in the absence (bottom) and presence (top) of TBACl ( $7.08 \times 10^{-3}$  M); (b) Negative ESI MS spectrum of  $^5,6F_4$ -FBimbe 12 ( $1.0 \times 10^{-3}$  M) in the presence of TBACl ( $7.08 \times 10^{-3}$  M) in acetonitrile.

The data in Table 1 firstly demonstrate that the FBimbe derivatives tend to exhibit higher activity than the corresponding Bimbe analogues. For example,  $^5F_2$ -FBimbe 9 is 6.9-fold more active than  $^5F_2$ -Bimbe 3. This suggests that fluorination of the central phenyl subunits boosts the activity, which is in agreement with our

previous finding that adding an electron-withdrawing group on the central phenyl subunit is favourable to the anionophoric activity.<sup>29</sup>

Secondly, the activity of these fluorinated derivatives relies on the total number of fluorine atoms on the benzimidazolyl and central

phenyl subunits. Specifically, increase in the number of fluorine atoms is favourable to the activity. This is supported from the finding that the nona-fluorinated  $^{4,5,6,7}F_8$ -FBimbe **13** having one fluorine atom on the central phenyl ring and four fluorine atoms on each terminal benzimidazolyl subunit exhibits the highest activity, 307-fold more active than the non-fluorinated Bimbe **1**. This result suggests that high-degree fluorination of the 1,3-bis(benzimidazol-2-yl)benzene core structure may serve as a practical strategy to enhance the transport efficiency.<sup>23</sup>

Thirdly, the location of fluorine atoms on the terminal benzimidazolyl subunits has limited effect on the activity. This is demonstrated by the finding that the compounds having the same total numbers, but different locations of fluorine atoms on the benzimidazolyl subunits, that is,  $^4F_2$ -Bimbe **2** vs  $^5F_2$ -Bimbe **3**,  $^4F_2$ -FBimbe **8** vs  $^5F_2$ -FBimbe **9**,  $^{4,5}F_4$ -Bimbe **4** vs  $^{4,6}F_4$ -Bimbe **5** vs  $^{5,6}F_4$ -Bimbe **6**, and  $^{4,5}F_4$ -FBimbe **10** vs  $^{4,6}F_4$ -FBimbe **11** vs  $^{5,6}F_4$ -FBimbe **12**,

exhibit similar ion transport activity.

Fourthly, the activity of these fluorinated bisbenzimidazolyl derivatives is largely regulated by the fluorination-induced lipophilicity rather than the anion binding affinity. It is known that fluorination boosts the activity of an anion transporter by increasing the anion-binding affinity and/or lipophilicity of the transporter molecule.<sup>22-25</sup> The data in Table 1 demonstrate that these compounds exhibit similar association constants with chloride anions, which rules out the possibility that anion-binding affinity is primarily responsible for the enhanced ion transport. Then we calculated the  $\text{clog}P$  values of these fluorinated compounds (Table 1) and analyzed the correlation between the  $\text{clog}P$  and  $\text{EC}_{50}$  values. As a consequence, it appears that the  $\text{EC}_{50}$  values decay exponentially with the  $\text{clog}P$  values (Fig. S79). This result demonstrates that the transport efficiency of these compounds is primarily regulated by the lipophilicity within the tested range.

Table 1. Lipophilicity ( $\text{clog}P$ ), association constants ( $K_a$ 's) and anion transport efficiency ( $\text{EC}_{50}$ )

Compound	$\text{clog}P^a$	Anion binding <sup>b</sup>		Ion transport (Pyranine Assay) <sup>c</sup>		
		$K_a$ ( $\text{M}^{-1}$ )	$\text{RA}_1^d$	n	$\text{EC}_{50}$ (mol%)	$\text{RA}_2^d$
Bimbe <b>1</b>	4.60	$(3.51 \pm 0.09) \times 10^3$	1.0	$2.06 \pm 0.06$	$9.67 \pm 0.89$	1.0
$^4F_2$ -Bimbe <b>2</b>	4.88	$(4.14 \pm 0.57) \times 10^3$	1.2	$1.14 \pm 0.07$	$3.16 \pm 0.23$	3.0
$^5F_2$ -Bimbe <b>3</b>	4.88	$(4.94 \pm 0.19) \times 10^3$	1.4	$0.91 \pm 0.25$	$3.61 \pm 0.09$	2.7
$^{4,5}F_4$ -Bimbe <b>4</b>	5.17	$(3.04 \pm 0.42) \times 10^3$	0.9	$0.98 \pm 0.06$	$0.62 \pm 0.07$	15.6
$^{4,6}F_4$ -Bimbe <b>5</b>	5.17	$(3.11 \pm 0.29) \times 10^3$	0.9	$1.04 \pm 0.22$	$0.21 \pm 0.06$	46.0
$^{5,6}F_4$ -Bimbe <b>6</b>	5.17	$(2.38 \pm 0.25) \times 10^3$	0.7	$1.03 \pm 0.18$	$0.31 \pm 0.05$	31.6
FBimbe <b>7</b>	4.74	$(5.40 \pm 0.08) \times 10^3$	1.5	$2.00 \pm 0.04$	$8.63 \pm 0.14$	1.1
$^4F_2$ -FBimbe <b>8</b>	5.02	$(1.40 \pm 0.29) \times 10^4$	4.0	$1.14 \pm 0.02$	$1.66 \pm 0.22$	5.8
$^5F_2$ -FBimbe <b>9</b>	5.02	$(5.01 \pm 0.21) \times 10^3$	1.4	$1.08 \pm 0.10$	$0.52 \pm 0.08$	18.6
$^{4,5}F_4$ -FBimbe <b>10</b>	5.31	$(9.84 \pm 0.54) \times 10^3$	2.8	$1.07 \pm 0.08$	$0.18 \pm 0.01$	53.7
$^{4,6}F_4$ -FBimbe <b>11</b>	5.31	$(8.91 \pm 0.53) \times 10^3$	2.5	$0.93 \pm 0.04$	$0.16 \pm 0.02$	60.4
$^{5,6}F_4$ -FBimbe <b>12</b>	5.31	$(6.92 \pm 0.47) \times 10^3$	2.0	$1.00 \pm 0.04$	$(6.46 \pm 1.31) \times 10^{-2}$	150
$^{4,5,6,7}F_8$ -FBimbe <b>13</b>	5.88	$(8.80 \pm 3.64) \times 10^3$	2.5	$0.92 \pm 0.07$	$(3.15 \pm 0.09) \times 10^{-2}$	307

<sup>a</sup> Calculated using MarvinSketch (Version 6.1.0, Weighted Model, ChemAxon, MA).

<sup>b</sup> Measured by means of  $^1\text{H}$  NMR titrations in  $\text{CD}_3\text{CN}$ . See Fig. S75 and Table S1 for the association constants measured in  $\text{CH}_3\text{CN}/\text{H}_2\text{O}$  (9/1, v/v) by means of spectrophotometric titrations.

<sup>c</sup> Measured under the intravesicular conditions: 0.1 mM pyranine in 25 mM HEPES (50 mM NaCl, pH 7.0) and extravesicular conditions: 25 mM HEPES (50 mM NaCl, pH 8.0).  $\lambda_{\text{ex}}$  460 nm/ $\lambda_{\text{em}}$  510 nm.

<sup>d</sup>  $\text{RA}_1$  and  $\text{RA}_2$  are the relative binding affinity and ion transport efficiency of each compound relative to Bimbe **1**, respectively.

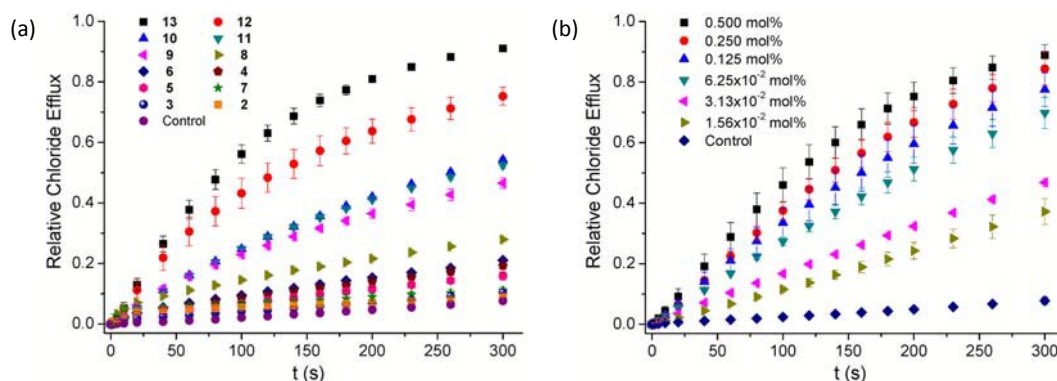
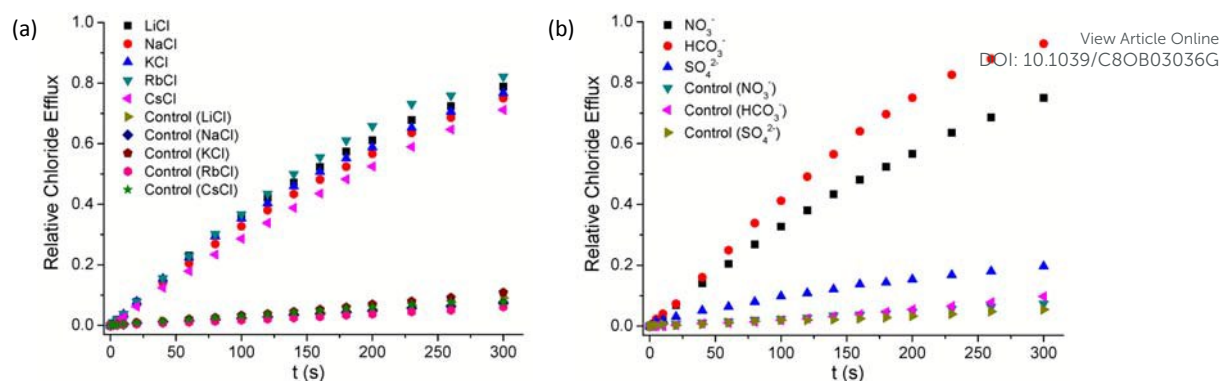
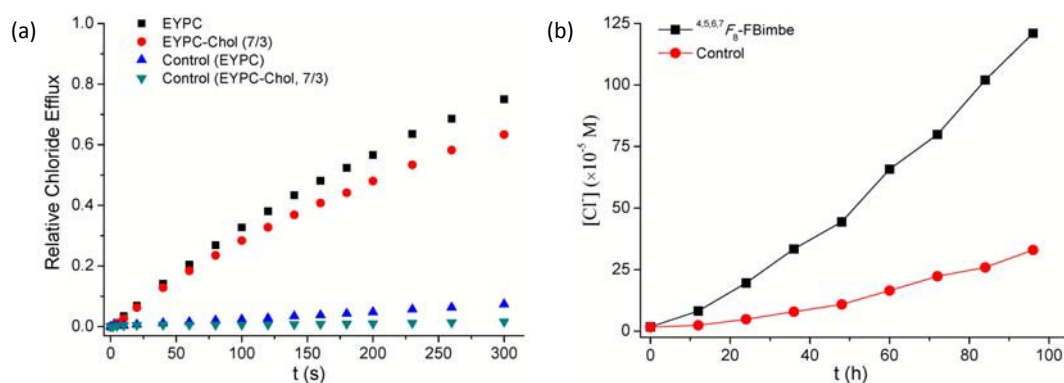


Fig. 3. Relative chloride efflux out of EYPC liposomes enhanced by (a) each compound (1 mol%) and (b)  $^{4,5,6,7}F_8$ -FBimbe **13** of varying concentrations. Intravesicular conditions: 500 mM NaCl in 25 mM HEPES buffer (pH 7.0); Extravesicular conditions: 500 mM  $\text{NaNO}_3$  in 25 mM HEPES buffer (pH 7.0).



**Fig. 4.** (a) Relative chloride efflux out of EYPC liposomes containing Li<sup>+</sup>, Na<sup>+</sup>, K<sup>+</sup>, Rb<sup>+</sup> or Cs<sup>+</sup>, enhanced by <sup>4,5,6,7</sup>F<sub>8</sub>-FBimbe **13** (0.125 mol%), under the intravesicular conditions: 500 mM MCl in 25 mM HEPES buffer (pH 7.0) and extravesicular conditions: 500 mM MNO<sub>3</sub> in 25 mM HEPES buffer (pH 7.0) (M = Li, Na, K, Rb or Cs). (b) Relative chloride efflux out of EYPC liposomes, enhanced by <sup>4,5,6,7</sup>F<sub>8</sub>-FBimbe **13** (0.125 mol%), under the intravesicular conditions: 500 mM NaCl in 25 mM HEPES buffer (pH 7.0) and extravesicular conditions: 500 mM NaNO<sub>3</sub>, 500 mM NaHCO<sub>3</sub> or 250 mM Na<sub>2</sub>SO<sub>4</sub> in 25 mM HEPES buffer (pH 7.0).



**Fig. 5.** (a) Relative chloride efflux out of EYPC (■) and EYPC/Chol (7/3, ●) liposomes, promoted by <sup>4,5,6,7</sup>F<sub>8</sub>-FBimbe **13** (0.125 mol%), under the intravesicular conditions: 500 mM NaCl in 25 mM HEPES buffer (pH 7.0) and extravesicular conditions: 500 mM NaNO<sub>3</sub> in 25 mM HEPES buffer (pH 7.0). (b) Chloride transport across a bulky nitrobenzene membrane, promoted by <sup>4,5,6,7</sup>F<sub>8</sub>-FBimbe **13** (1.0 mM) and detected by a chloride ion selective electrode in the receiving aqueous phase of U-tube.

**Anion selective transport.** To assess the anion-selective transport activity of these compounds, we measured their ability to facilitate the efflux of chloride anions out of the EYPC liposomes by means of chloride ion selective electrode techniques (Fig. 3 and S80).<sup>36</sup> The concentration-dependent chloride efflux indicates that these compounds are capable of mediating the transport of chloride anions across lipid bilayers. Similar as observed in pH discharge assays, the FBimbe derivatives **7-13** tend to exhibit higher chloride efflux activity than the corresponding Bimbe analogues **1-6**. It is noteworthy that the EC<sub>50, 260 s</sub> values are much higher than those obtained from the pH discharge experiments (Table S3), suggesting that pyranine assay is a much more sensitive approach for probing the ion transport properties of an anion transporter.<sup>37,38</sup>

To gain further insights into the anion selectivity and the probable mechanism of action, we measured the chloride efflux activity of these fluorinated compounds in the presence of different alkali metal ions or anions (Fig. 4 and Fig. S81-S82). The chloride efflux activity is independent on the alkali metal ions, but varies with the tested anions. These results indicate that Cl<sup>-</sup>/NO<sub>3</sub><sup>-</sup> antiport and/or H<sup>+</sup>/Cl<sup>-</sup> symport may be involved during the chloride efflux.<sup>39</sup> The chloride efflux activity was found to be significantly suppressed by

highly hydrophilic sulfate anions and be recovered by carbonate anions, strongly suggesting that anion exchange is the primary mode of action.<sup>36,40</sup>

**Probable mechanism of action** As <sup>4,5,6,7</sup>F<sub>8</sub>-FBimbe **13** is the most active, we measured its chloride efflux out of 30% cholesterol (Chol)-containing EYPC vesicles to probe the probable mechanism of action (Fig. 5a and Fig. S83). The observed reduction in the chloride efflux implies that <sup>4,5,6,7</sup>F<sub>8</sub>-FBimbe **13** may function as a mobile carrier.<sup>23</sup> To further confirm this probable mechanism, we carried out a U-tube assay (Fig. 5b).<sup>23</sup> In this experiment, a bulky nitrobenzene membrane was used to separate a sodium chloride solution as the resource phase from a sodium nitrate solution as the receiving phase. The transport of chloride anions through the nitrobenzene phase was monitored by using a chloride ion selective electrode. Compared with the blank, addition of <sup>4,5,6,7</sup>F<sub>8</sub>-FBimbe **13** led to a higher concentration of chloride anions in the receiving phase. This result in combination with the reduced chloride efflux observed by the cholesterol assay, suggests that <sup>4,5,6,7</sup>F<sub>8</sub>-FBimbe **13** mediates the transmembrane transport of anions most probably via a mobile carrier mechanism.

Taken together, the above observations suggest that these fluorinated compounds function as highly effective anion-selective carriers primarily through a process of anion exchange.

#### *In vitro* anion transport

Inspired by the potent transport activity of these compounds on liposomal models, we chose four compounds, that is, FBimbe **7**,  $^5F_2$ -FBimbe **9**,  $^{5,6}F_4$ -FBimbe **12** and  $^{4,5,6,7}F_8$ -FBimbe **13** to investigate their anionophoric activity in live cells.

**Acridine orange staining** Firstly, we carried out vital staining on HeLa cervical cancer cells by using cell-permeable acridine orange (AO). It is known that AO emits characteristic orange fluorescence

in acidic compartments such as lysosomes, and green fluorescence when the acidic compartments are basified. As shown in Fig. 6a, when HeLa cells were stained with AO, scattered orange fluorescence was observed in the cytoplasm, suggesting that AO is located in acidic organelles. Treatment of the HeLa cells with FBimbe **7** and  $^5F_2$ -FBimbe **9** led to partial reduction in the orange emission (Fig. 6b and c), and with  $^{5,6}F_4$ -FBimbe **12** and  $^{4,5,6,7}F_8$ -FBimbe **13** led to complete loss of the orange emission (Fig. 6d and e). This result suggests that these compounds are able to basify the acidic organelles, in the same order observed in liposomal models. The  $\text{Cl}^-/\text{HCO}_3^-$  antiport observed in the liposomal experiments may be responsible for the increase of the internal pH.<sup>14-19, 29</sup>

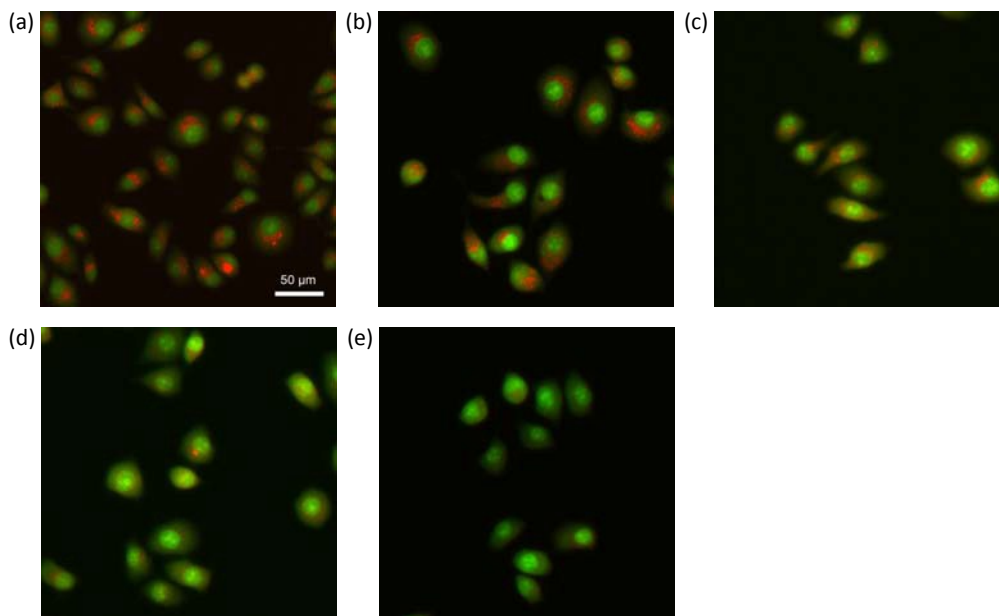


**Fig. 6.** Acridine orange staining of HeLa cells. (a) Untreated cells (control); (b)-(e) cells treated with 10  $\mu\text{M}$  of (b) FBimbe **7**, (c)  $^5F_2$ -FBimbe **9**, (d)  $^{5,6}F_4$ -FBimbe **12** and (e)  $^{4,5,6,7}F_8$ -FBimbe **13**, respectively, for 1.5 h.

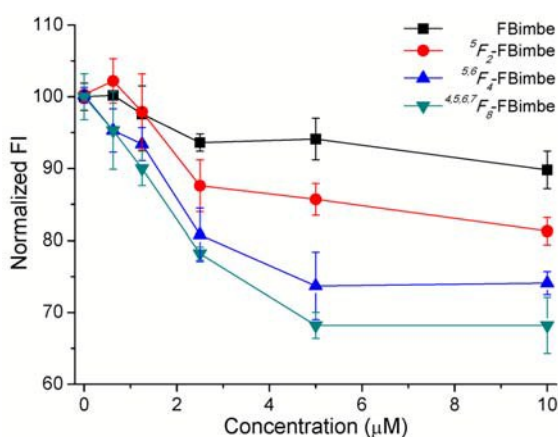


**Fig. 7.** Normalized fluorescent intensity of MQAE in HeLa cells incubated with MQAE (5 mM) for 3.5 h followed by the treatment with FBimbe **7** ( $\blacksquare$ ),  $^5F_2$ -FBimbe **9** ( $\bullet$ ),  $^{5,6}F_4$ -FBimbe **12** ( $\blacktriangle$ ) and  $^{4,5,6,7}F_8$ -FBimbe **13** ( $\blacktriangledown$ ) of varying concentrations for 2 h. Fluorescent intensity was recorded by the plate reader at  $\lambda_{\text{em}} = 460$  nm ( $\lambda_{\text{ex}} = 350$  nm), and normalized with respect to the fluorescent intensity of untreated cells. Each data point represents the mean

intensity of three independent experiments.

**MQAE assay** Similar to pH discharge experiments, AO staining does not provide any evidence for whether these compounds are able to facilitate the influx of anions into cells. To clarify this, we investigated the ability of FBimbe **7**,  $^5F_2$ -FBimbe **9**,  $^{5,6}F_4$ -FBimbe **12** and  $^{4,5,6,7}F_8$ -FBimbe **13** to mediate the entry of chloride anions into HeLa cells by using a fluorescent assay based on *N*-(ethoxycarbonylmethyl)-6-methoxyquinolinium bromide (MQAE).<sup>14-19, 29</sup> Because MQAE is a cell-permeable, chloride selective dye, its fluorescence quenching upon the treatment of the HeLa cells with FBimbe **7**,  $^5F_2$ -FBimbe **9**,  $^{5,6}F_4$ -FBimbe **12** or  $^{4,5,6,7}F_8$ -FBimbe **13** may serve as a direct evidence that these compounds are involved in the influx of chloride anions into the HeLa cells. As shown in Fig. 7, post incubation of the HeLa cells with FBimbe **7**,  $^5F_2$ -FBimbe **9**,  $^{5,6}F_4$ -FBimbe **12** and  $^{4,5,6,7}F_8$ -FBimbe **13** led to significant quenching of the MQAE fluorescence. This result clearly indicates that these compounds are able to mediate the influx of chloride anions into the intracellular matrix.

#### Biological activity

**Cytotoxicity.** It is well recognized that facilitated transport of

chloride anions across cells may induce cell death.<sup>20,26,29</sup> The ability of these fluorinated derivatives to mediate the transport of chloride anions into live cells inspired us to test their *in vitro* cytotoxicity toward four solid tumor cells, including HeLa, A549 lung adenocarcinoma, MCF-7 breast and HepG2 human liver cancer cells. Initially, we screened the anti-proliferative activity of all the compounds at the concentration of 50  $\mu$ M and then measured their IC<sub>50</sub> values, by using a conventional MTT [3-(4,5-dimethylthiazol-2-yl)-2,5-diphenyltetrazolium bromide] assay. Here the IC<sub>50</sub> value represents the concentration of each compound resulting in 50% inhibition in cell growth. The cell viability expressed as a percentage of control cells is shown in Fig. 8 and Table S4, and the IC<sub>50</sub> values are reported in Fig. S85-S96, Table 2 and Tables S5-S6. For comparison, the IC<sub>50</sub> values of all the compounds toward LO2 human normal liver cells were also measured (Fig. S85-S96, Table 2 and Table S7). Doxorubicin was used as a positive control.

The data in Table 2 demonstrate that in general, the FBimbe series tend to exhibit higher cytotoxicity than the corresponding Bimbe series, which suggests that fluorination of the central phenyl rings is favourable not only to the anion transport but also to the cytotoxic effect. Interestingly, the location of fluorine atoms on the benzimidazolyl subunits has an obvious impact on the cytotoxicity.

Specifically, fluorination at the 4- or 7-position of the benzimidazolyl subunits is not favorable to the cytotoxicity. Thus, the compounds having significant anion transport, such as <sup>5,6</sup>F<sub>4</sub>-FBimbe **12** and <sup>4,5,6,7</sup>F<sub>8</sub>-FBimbe **13** exhibit potent cytotoxicity. In addition, no discrimination between cancerous and normal cells is observed.

#### Probable mechanism of biological action

**Effect of chloride anions on the cytotoxicity** It is reported that dysregulation of ion homeostasis, in particular *via* chloride influx into cells, can induce cell shrinkage and lead to apoptosis.<sup>20,26,42,43</sup>

As shown above, these fluorinated compounds are able to facilitate the entry of chloride anions into live cells, and their cytotoxicity parallels their *in vitro* anionophoric activity. These results imply that chloride transport across cellular membranes may be responsible for the cytotoxic effects. To gain support for this, we measured the cytotoxicity of <sup>5,6</sup>F<sub>4</sub>-FBimbe **12** and <sup>4,5,6,7</sup>F<sub>8</sub>-FBimbe **13** toward HeLa cells in the presence and absence of chloride anions. As shown in Fig. 9a-b, both <sup>5,6</sup>F<sub>4</sub>-FBimbe **12** and <sup>4,5,6,7</sup>F<sub>8</sub>-FBimbe **13** were more cytotoxic in the presence of chloride anions than in the absence of chloride anions. This result strongly suggests that chloride transport may be one of the major factors that are responsible for the cytotoxic effects.

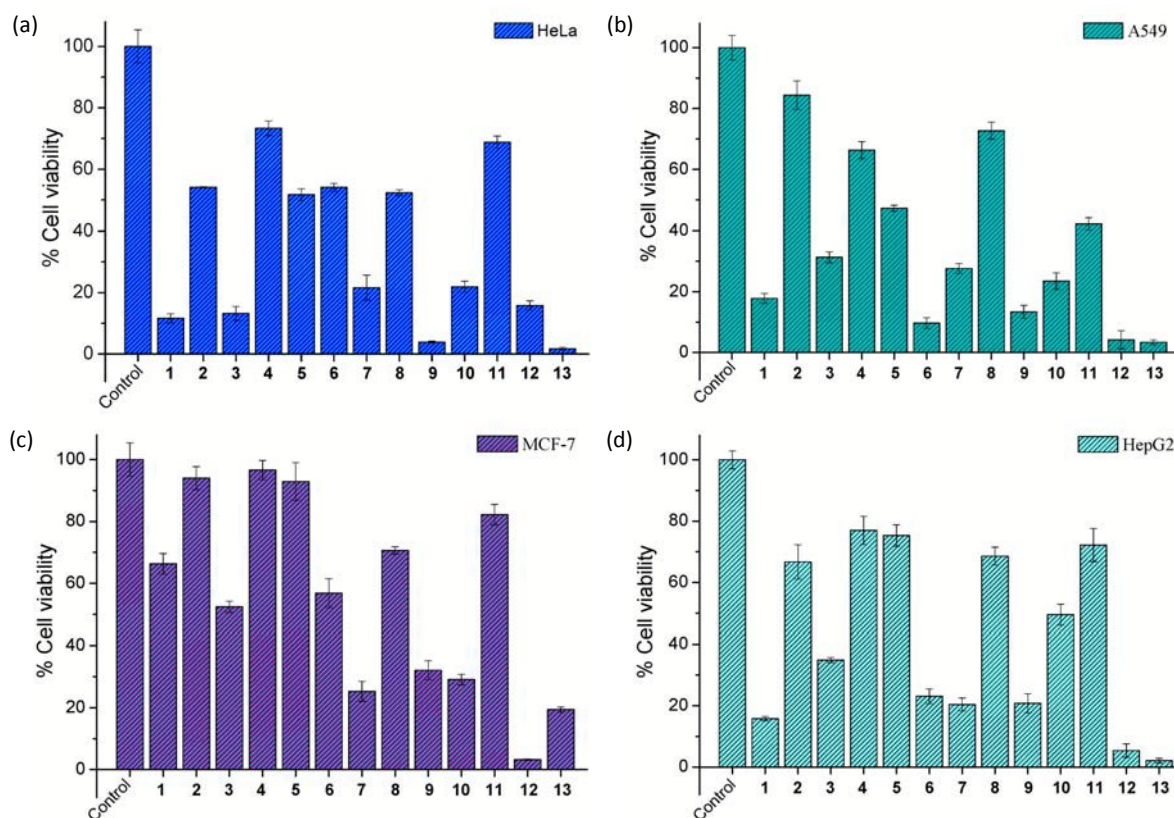


Fig. 8. Cell viability of Bimbe **1** and the fluorinated derivatives **2-13** (50  $\mu$ M) toward (a) HeLa, (b) A549, (c) MCF-7 and (d) HepG2 cancer cells.

Table 2. Anionophoric activity (EC<sub>50</sub>, μM) and cytotoxicity (IC<sub>50</sub>, μM) of Bimbe **1** and the fluorinated derivatives **2-13**.

Compound	EC <sub>50</sub> (μM) <sup>a</sup>	IC <sub>50</sub> (μM) <sup>b</sup>				
		HeLa	A549	MCF-7	HepG-2	LO2
Bimbe <b>1</b>	17.0±1.60	12.5±1.2	18.8±1.6	> 50	12.4±0.7	16.8±0.9
<sup>4</sup> F <sub>2</sub> -Bimbe <b>2</b>	5.55±0.41	> 50	> 50	> 50	> 50	> 50
<sup>5</sup> F <sub>2</sub> -Bimbe <b>3</b>	6.34±0.16	6.2±0.3	22.2±4.0	> 50	20.5±0.8	18.8±0.3
<sup>4,5</sup> F <sub>4</sub> -Bimbe <b>4</b>	1.08±0.11	> 50	> 50	> 50	> 50	> 50
<sup>4,6</sup> F <sub>4</sub> -Bimbe <b>5</b>	0.38±0.10	> 50	36.6±4.7	> 50	> 50	> 50
<sup>5,6</sup> F <sub>4</sub> -Bimbe <b>6</b>	0.54±0.09	> 50	6.2±0.2	> 50	9.8±0.8	30.2±3.1
FBimbe <b>7</b>	15.2±0.20	15.1±4.0	21.6±1.1	37.8±2.3	28.2±1.6	26.1±4.1
<sup>4</sup> F <sub>2</sub> -FBimbe <b>8</b>	2.91±0.39	47.3±4.4	> 50	> 50	> 50	> 50
<sup>5</sup> F <sub>2</sub> -FBimbe <b>9</b>	0.91±0.14	5.6±0.2	5.8±0.7	21.0±1.5	10.6±0.9	8.3±0.6
<sup>4,5</sup> F <sub>4</sub> -FBimbe <b>10</b>	0.32±0.01	6.5±1.3	4.5±0.8	15.7±0.8	44.0±4.3	6.3±1.3
<sup>4,6</sup> F <sub>4</sub> -FBimbe <b>11</b>	0.28±0.04	> 50	8.7±0.1	> 50	> 50	> 50
<sup>5,6</sup> F <sub>4</sub> -FBimbe <b>12</b>	0.11±0.02	7.6±2.2	3.2±0.6	4.6±0.8	6.3±0.1	4.1±0.3
<sup>4,5,6,7</sup> F <sub>8</sub> -FBimbe <b>13</b>	(5.54±0.16)×10 <sup>-2</sup>	3.8±0.1	4.0±0.4	11.4±0.6	2.6±0.6	3.4±0.5
Doxorubicin	/	0.16±0.06	0.46±0.04	0.15±0.01	2.5±0.3	0.14±0.01

<sup>a</sup> Calculated by multiplying the EYPC concentrations (1.76×10<sup>-4</sup> M) of EYPC by the EC<sub>50</sub> values (in mol%) of each compound listed in Table 1.

<sup>b</sup> > 50 μM means that the cell viability tested at 50 μM was > 50% (Fig. 8).

**Effect of necrotic, apoptotic and autophagic inhibitors on the cytotoxicity** According to the morphological characteristics and biochemical markers, cell death may be divided into several categories, mainly including necrosis, apoptosis and autophagy.<sup>44</sup> To clarify which one is responsible for the cell death induced by these fluorinated compounds, we measured the cytotoxicity of <sup>5,6</sup>F<sub>4</sub>-FBimbe **12** and <sup>4,5,6,7</sup>F<sub>8</sub>-FBimbe **13** toward HeLa cells in the presence of a necrotic inhibitor Nec-1, an autophagic inhibitor 3-MA or an apoptotic inhibitor Z-VAD-FMK (Fig. 9c and Fig. S97-S99). As a result, the cell viability was not recovered after the administration of Nec-1 or 3-MA, ruling out the possibility that the cell death proceeds *via* a process of necrosis or autophagy. Though it is reported that synthetic anion transporters are able to disrupt the autophagy of cells,<sup>26</sup> the present finding suggests that the formation and accumulation of autophagosomes are not crucial for the cytotoxic effects of these fluorinated bisbenzimidazolyl derivatives. However, administration of Z-VAD-FMK led to significant recovery in the cell viability. This result suggests that the cell death triggered by <sup>5,6</sup>F<sub>4</sub>-FBimbe **12** and <sup>4,5,6,7</sup>F<sub>8</sub>-FBimbe **13** may proceed *via* an apoptotic pathway. This probable mechanism of apoptosis was further confirmed by means of Hoechst 33342 and JC-1 staining of HeLa cells.

**Hoechst 33342 staining** It is known that Hoechst 33342 staining may be used to differentiate apoptosis from other cell death mechanisms through morphological observation.<sup>16,19</sup> As shown in Fig. 10, compared with the untreated cells, the cells treated with FBimbe **7**, <sup>5</sup>F<sub>2</sub>-FBimbe **9**, <sup>5,6</sup>F<sub>4</sub>-FBimbe **12** or <sup>4,5,6,7</sup>F<sub>8</sub>-FBimbe **13** exhibit stronger blue fluorescence, indicative of chromatin condensation, fragmentation and apoptotic bodies formation. The formation of “bean”-shaped nuclei was also observed. These are typical features for cell death *via* an apoptotic process.<sup>16,17,19</sup>

**JC-1 staining** The reduction of mitochondrial membrane potential is a hallmark of apoptosis,<sup>16,17</sup> and this may be monitored by a cell-permeable dye JC-1 the fluorescence of which is sensitive to

mitochondrial membrane potential.<sup>45</sup> As shown in Fig. 11 and Fig. S100, treatment of the HeLa cells with <sup>5,6</sup>F<sub>4</sub>-FBimbe **12** or <sup>4,5,6,7</sup>F<sub>8</sub>-FBimbe **13** of varying concentrations and then with JC-1 led to a significant change in the fluorescence of JC-1 from red to green. This is indicative of a decrease in the mitochondrial membrane potential and is one of the characteristics for apoptotic cell death at an early stage.<sup>16,17</sup>

### 3. Conclusions

In conclusion, we have successfully synthesized a series of fluorinated bisbenzimidazolyl derivatives and systematically studied their anion recognition, transmembrane anion transport, cytotoxicity and probable mechanism of biological action.<sup>1</sup> <sup>1</sup>H NMR titrations and ESI MS spectrometric detections indicate that these compounds are able to form stable complexes with chloride anions. These compounds exhibit potent anion transport in liposomal models, and the anionophoric activity may be regulated by the total number of fluorine atoms. MQAE assay and AO vital staining indicate that these compounds are able to disturb the homeostasis of chloride anions, modify the intracellular pH and induce the basification of acidic lysosomes. MTT assays indicate that most of these fluorinated bisbenzimidazolyl derivatives exhibit potent cytotoxicity toward the selected four solid tumor cells, and the derivatives having one fluorine atom on the central phenyl ring and two or four fluorine atoms on each terminal benzimidazolyl subunit have the IC<sub>50</sub> values in the low micromolar range. The higher cytotoxicity in the presence of chloride anions suggests that the transport of chloride anions across the cellular membranes plays a critical role in the cytotoxic effects. Mechanistic study based on necrotic, apoptotic or autophagic inhibitors, Hoechst 33342 and JC-1 staining suggests that these compounds trigger cell death most probably *via* an apoptotic process. The present findings together with the drug-like features of these fluorinated compounds strongly suggest that they are exploitable as apoptotic agents for cancers. Further investigations into the probable mechanism of action are

presently under progress, with the aim to develop potential anti-cancer chemotherapeutic agents that exert their activity by

disordering the ion homeostasis of cancer cells.

View Article Online  
DOI: 10.1039/C8OB03036G

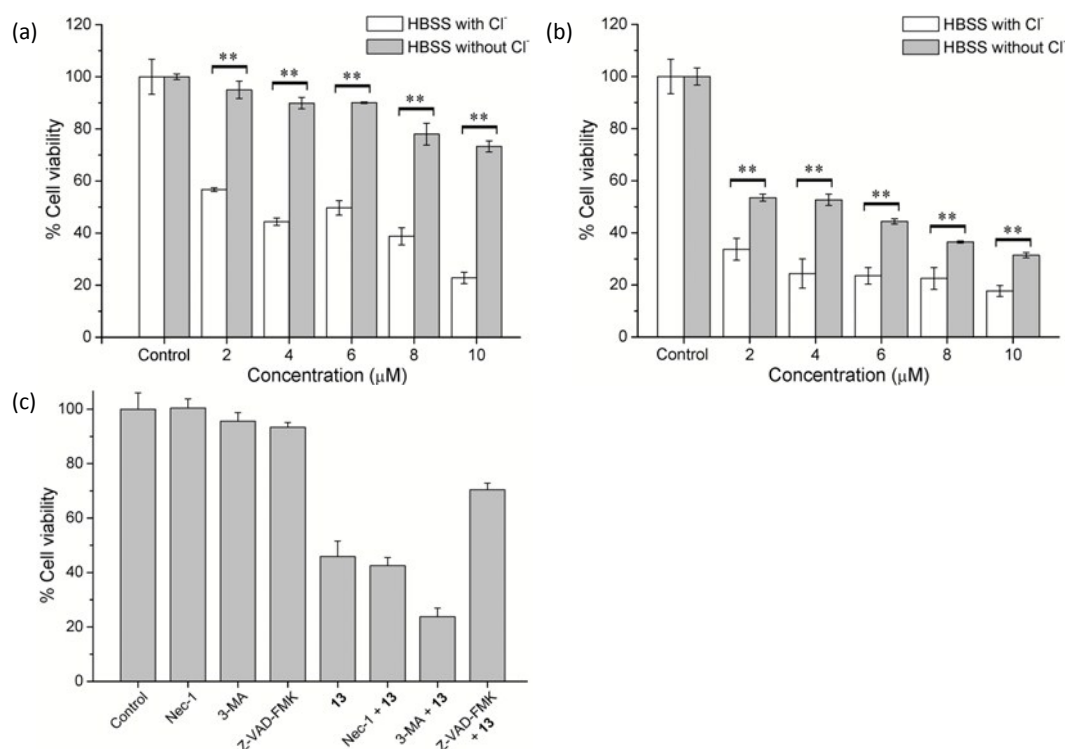


**Fig. 9.** (a, b) Viability of HeLa cells in the presence and absence of chloride anions in extracellular media (HBSS buffer) upon the dose-dependent treatment of <sup>5,6</sup>F<sub>4</sub>-FBimbe **12** (a, 18 h) and <sup>4,5,6,7</sup>F<sub>8</sub>-FBimbe **13** (b, 24 h) (mean ± s.d., n = 4, \*\*P < 0.01, Independent-Sample T Test). (c) Viability of HeLa cells incubated with Nec-1 (25 μM), 3-MA (2.0 mM) or Z-VAD-FMK (25 μM) for 2 h, followed by the treatment with <sup>4,5,6,7</sup>F<sub>8</sub>-FBimbe **13** (10 μM) for 24 h.

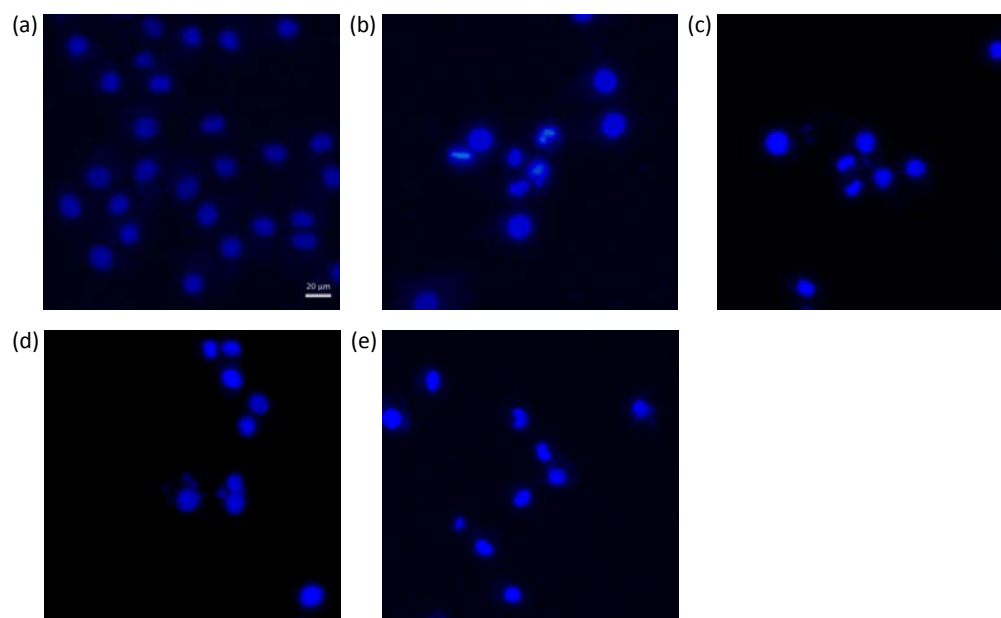


**Fig. 10.** Hoechst 33342 staining of HeLa cells. (a) Untreated cells; (b)-(e) cells treated with 10 μM of (b) FBimbe **7**, (c) <sup>5</sup>F<sub>2</sub>-FBimbe **9**, (d) <sup>5,6</sup>F<sub>4</sub>-FBimbe **12** and (e) <sup>4,5,6,7</sup>F<sub>8</sub>-FBimbe **13** for 24 h, respectively.

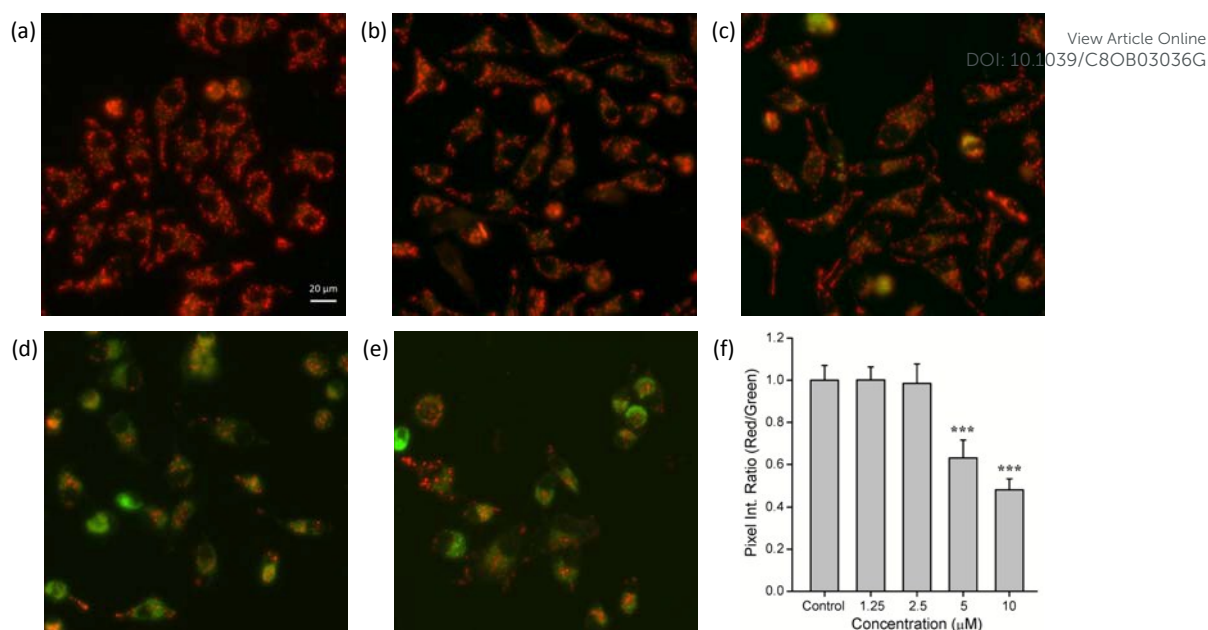


**Fig. 11.** JC-1 staining of HeLa cells. (a) Untreated (control) cells; (b)–(e) cells treated with  $^{4,5,6,7}F_8$ -FBimbe **13** at the concentrations of 1.25  $\mu\text{M}$ , 2.5  $\mu\text{M}$ , 5  $\mu\text{M}$  and 10  $\mu\text{M}$ , respectively; (f) Pixel ratio (red/green) for different concentrations of  $^{4,5,6,7}F_8$ -FBimbe **13**, analysed by ImageJ (mean  $\pm$  s.d.,  $n = 9$ , \*\*\* $P < 0.001$ , Independent-Sample T Test).

#### 4. Experimental

**Generals.** A Bruker Avance AV 400 NMR spectrometer was used to measure the  $^1\text{H}$  and  $^{13}\text{C}$  NMR spectra, and the data were reported relative to the deuterium solvents. Waters UPLC/Quattro Premier XE and Bruker maXis 4G ESI-Q-TOF mass spectrometers were used to measure the LR and HR ESI-MS spectra, respectively. Melting points (mp) were measured on an X-5 micro melting point apparatus. Analytical thin-layer chromatography (TLC) plates (silica gel, GF254) were detected by use of iodine and UV (254 or 365 nm). EYPC vesicles were prepared by extrusion through nucleopore track-etched polycarbonate membranes (100 nm, Whatman, Florham Park, New Jersey, USA) on an Avanti's Mini-Extruder (Avanti Polar Lipids, Inc., Alabaster, Alabama, USA). Chloride efflux was measured by using a Mettler-Toledo Perfection<sup>TM</sup> chloride ion selective electrode assembled with a Mettler-Toledo Seven Compact S220 ionometer. Ultraviolet–visible and Fluorescence spectra were measured on a Perkin Elmer Lambda 25 spectrophotometer and Perkin Elmer LS55 spectrofluorimeter, respectively. MTT-based cytotoxicity assay and MQAE assays were measured on a Tecan Infinite M1000 PRO microplate reader. Acridine orange, Hoechst 33342 and JC-1 staining experiments were carried out on a Carl Zeiss Axio Observer A1 microscope.

EYPC and pyranine were purchased from Sigma Chemical Co. (St Louis, USA). Calcein, cholesterol, acridine orange and Hoechst 33342 were purchased from J&K Chemical Co. (Beijing, China). MTT was supplied by Amresco (Ohio, USA). MQAE and 3-MA were supplied by Aladdin (Shanghai, China). JC-1 mitochondrial membrane potential detection kit was supplied by Genview (Florida, USA). Nec-1 and Z-VAD-FMK were purchased from Selleck (Houston, USA) and Apexbio (Houston, USA), respectively. Bimbe **1** and  $^5F_2$ -Bimbe **3** were prepared according to the protocols reported by us and others.<sup>28,31</sup> All the other chemicals and reagents were obtained

from commercial sources and used without further purification.

#### Synthesis of 5-fluoro-benzene-1,3-dicarbaldehyde

A solution of 1-fluoro-3,5-dimethyl-benzene (1.3 mL, 10.8 mmol), NBS (11.4 g, 64.7 mmol) and AIBN (1.10 g, 6.70 mmol) in  $\text{CCl}_4$  (70 mL) was refluxed for 8 h. The mixture was filtered and the filtrate was concentrated under reduced pressure. The residue was dissolved in concentrated sulfuric acid (30 mL). The resulting mixture was heated at 110  $^\circ\text{C}$  for 1 d, and then added drop wise into iced water (50 mL). The mixture was extracted with ethyl ether (100 mL $\times$ 3). The ether layer was washed subsequently with saturated  $\text{Na}_2\text{CO}_3$  solution (100 mL $\times$ 3) and saline (100 mL $\times$ 3), and dried over anhydrous sodium sulfate. Purification was accomplished by re-crystallization from petroleum ether (b. p. 60–90  $^\circ\text{C}$ ) to afford 5-fluoro-benzene-1,3-dicarbaldehyde (181 mg, 11%) having negative ESI-MS:  $m/z$  151.62 ( $[\text{M}-\text{H}]^-$ );  $^1\text{H}$  NMR ( $\text{CDCl}_3$ , 400 MHz)  $\delta$  10.09 (s, 2H), 8.20 (t,  $J = 1.2$  Hz, 1H), 7.84 (dd,  $J = 1.2$  and 7.8 Hz, 2H) and  $^{13}\text{C}$  NMR ( $\text{CDCl}_3$ , 100 MHz)  $\delta$  189.6 ( $\times 2$ ), 163.5 (d,  $J = 252.0$  Hz), 139.0 (d,  $J = 5.9$  Hz), 127.0 ( $\times 2$ ), 120.9 (d,  $J = 22.4$  Hz). The  $^1\text{H}$  and  $^{13}\text{C}$  NMR data were in agreement with the reported ones in literature.<sup>32</sup>

#### Synthesis of $^4F_2$ -Bimbe **2**

A solution of 1,3-benzenedialdehyde (51 mg, 0.38 mmol) and 3-fluoro-1,2-benzenediamine (115 mg, 0.92 mmol) in DMSO (1.5 mL) was stirred at room temperature. The reaction was monitored with TLC ( $\text{CHCl}_3/\text{CH}_3\text{OH}$ , 20/1, v/v). After 48 h, the reaction solution was added to water (200 mL). The resulting precipitates were collected through filtration and purified by preparative TLC ( $\text{CHCl}_3/\text{CH}_3\text{OH}$ , 15/1, v/v) to give  $^4F_2$ -Bimbe **2** (42 mg, 32%) having mp 271.1–272.3  $^\circ\text{C}$ ;  $^1\text{H}$  NMR ( $\text{DMSO}-d_6$ , 400 MHz)  $\delta$  9.02 (s, 1H), 8.41 (d,  $J = 7.6$  Hz, 2H), 7.76 (t,  $J = 8.0$  Hz, 1H), 7.45 (d,  $J = 7.6$  Hz, 2H), 7.23 (m, 2H), 7.04 (m, 2H);  $^{13}\text{C}$  NMR ( $\text{DMSO}-d_6$ , 100 MHz)  $\delta$  151.8, 130.9, 130.1,

128.6, 125.6, 123.4 (d,  $J = 5.7$  Hz), 107.6 (d,  $J = 16.7$  Hz); ESI-MS:  $m/z$  347.80 ([M+H]<sup>+</sup>), 369.54 ([M+Na]<sup>+</sup>) and HR-ESI-MS for C<sub>20</sub>H<sub>13</sub>F<sub>2</sub>N<sub>4</sub> ([M+H]<sup>+</sup>) Calcd: 347.1103; Found: 347.1100.

#### Synthesis of <sup>4,5</sup>F<sub>4</sub>-Bimbe 4

A solution of 1,3-benzenedialdehyde (51 mg, 0.38 mmol) and 3,4-difluoro-1,2-benzenediamine (132 mg, 0.92 mmol) in DMSO (3.0 mL) was heated at 80 °C. The reaction was monitored with TLC (CHCl<sub>3</sub>/CH<sub>3</sub>OH, 20/1, v/v). After 36 h, the reaction solution was added to water (200 mL). The resulting precipitates were collected through filtration and washed with methanol thrice to afford <sup>4,5</sup>F<sub>4</sub>-Bimbe 4 (114 mg, 80%) having mp > 300 °C; <sup>1</sup>H NMR (DMSO-*d*<sub>6</sub>, 400 MHz) δ 13.56 (br, 2H), 9.06 (s, 1H), 8.32 (dd,  $J = 7.6$  and 1.2 Hz, 2H), 7.79 (t,  $J = 7.6$  Hz, 1H), 7.41 (d, 2H,  $J = 5.2$  Hz), 7.30 (m, 2H); <sup>13</sup>C NMR (DMSO-*d*<sub>6</sub>, 100 MHz) δ 153.1, 145.9 (d,  $J = 233.2$  Hz), 145.8 (d,  $J = 233.5$  Hz), 130.6, 130.2, 128.7, 125.5, 112.3 (d,  $J = 20.7$  Hz); ESI-MS:  $m/z$  383.64 ([M+H]<sup>+</sup>), 405.58 ([M+Na]<sup>+</sup>) and HR-ESI-MS for C<sub>20</sub>H<sub>11</sub>F<sub>4</sub>N<sub>4</sub> ([M+H]<sup>+</sup>) Calcd: 383.0914; Found: 383.0913.

#### Synthesis of <sup>4,6</sup>F<sub>4</sub>-Bimbe 5

A solution of 1,3-benzenedialdehyde (51 mg, 0.38 mmol) and 3,5-difluoro-1,2-benzenediamine (134 mg, 0.93 mmol) in DMSO (3 mL) was stirred at room temperature. The reaction was monitored with TLC (CHCl<sub>3</sub>/CH<sub>3</sub>OH, 20/1, v/v). After 48 h, the reaction solution was added to water (200 mL). The resulting precipitates were collected through filtration and purified by chromatography on a silica-gel column, eluted with a mixture of CHCl<sub>3</sub>/CH<sub>3</sub>OH (110/1, v/v) to afford <sup>4,6</sup>F<sub>4</sub>-Bimbe 5 (56 mg, 38%) having mp > 300 °C; <sup>1</sup>H NMR (DMSO-*d*<sub>6</sub>, 400 MHz) δ 13.58 (br, 2H), 8.29 (d,  $J = 7.6$  Hz, 2H), 7.77 (t,  $J = 8.0$  Hz, 1H), 7.26 (d,  $J = 7.6$  Hz, 2H), 7.10 (t,  $J = 10.4$  Hz, 2H); <sup>13</sup>C NMR (DMSO-*d*<sub>6</sub>, 100 MHz) δ 158.7 (dd,  $J = 236.8, 10.8$  Hz), 152.9 (dd,  $J = 251.4$  and 16.3 Hz), 152.3, 137.7 (dd,  $J = 15.3$  and 11.1 Hz), 130.6, 130.2, 129.4 (d,  $J = 15.7$  Hz), 128.5, 125.1, 97.9 (dd,  $J = 28.5$  and 23.2 Hz), 95.0 (d,  $J = 25.7$  Hz); negative ESI-MS:  $m/z$  381.62 ([M-H]<sup>-</sup>) and negative HR-ESI-MS for C<sub>20</sub>H<sub>9</sub>F<sub>4</sub>N<sub>4</sub> ([M-H]<sup>-</sup>) Calcd: 381.0769; Found: 381.0776.

#### Synthesis of <sup>5,6</sup>F<sub>4</sub>-Bimbe 6

A solution of 1,3-benzenedialdehyde (51 mg, 0.38 mmol) and 4,5-difluoro-1,2-benzenediamine (130 mg, 0.90 mmol) in DMSO (6 mL) was stirred at room temperature. The reaction was monitored with TLC (CHCl<sub>3</sub>/CH<sub>3</sub>OH, 20/1, v/v). After 48 h, the reaction solution was added to water (200 mL). The resulting precipitates were collected through filtration and washed with methanol thrice to give <sup>5,6</sup>F<sub>4</sub>-Bimbe 6 (53 mg, 37%) having mp > 300 °C; <sup>1</sup>H NMR (DMSO-*d*<sub>6</sub>, 400 MHz) δ 8.99 (s, 1H), 8.25 (dd,  $J = 7.6$  and 1.2 Hz, 2H), 7.70-7.66 (m, 4H), 7.52 (t,  $J = 7.6$  Hz, 1H); <sup>13</sup>C NMR (DMSO-*d*<sub>6</sub>, 100 MHz) δ 153.0, 147.4 (d,  $J = 237.6$  and 15.7 Hz), 130.8, 130.1, 128.1, 125.1, 103.4, 103.0; negative ESI-MS:  $m/z$  381.68 ([M-H]<sup>-</sup>) and HR-ESI-MS for C<sub>20</sub>H<sub>9</sub>F<sub>4</sub>N<sub>4</sub> ([M-H]<sup>-</sup>) Calcd: 381.0769; Found: 381.0773.

#### Synthesis of FBimbe 7

A solution of 5-fluoro-benzene-1,3-dicarbaldehyde (51 mg, 0.33 mmol) and *o*-phenylenediamine (88 mg, 0.81 mmol) in CH<sub>3</sub>CN (3.0 mL) was refluxed. The reaction was monitored with TLC (CHCl<sub>3</sub>/CH<sub>3</sub>OH, 20/1, v/v). After 48 h, the reaction solution was concentrated under reduced pressure. The obtained residue was

purified with preparative TLC (CHCl<sub>3</sub>/CH<sub>3</sub>OH, 15/1, v/v) to give FBimbe 7 (54 mg, 49%) having mp 272.9-273.5 °C; <sup>1</sup>H NMR (DMSO-*d*<sub>6</sub>, 400 MHz) δ 13.57 (br, 1H), 9.03 (s, 1H), 8.19 (d,  $J = 9.6$  Hz, 2H), 7.73 (d,  $J = 4.8$  Hz, 2H), 7.61 (d,  $J = 6.0$  Hz, 2H), 7.27 (br, 4H); <sup>13</sup>C NMR (DMSO-*d*<sub>6</sub>, 100 MHz) δ 163.1 (d,  $J = 242.0$  Hz), 150.0 (×2), 143.9, 135.5, 133.5 (d,  $J = 9.0$  Hz), 123.5, 122.5, 121.3, 119.5, 114.5 (d,  $J = 23.8$  Hz), 112.2; ESI-MS:  $m/z$  329.91 ([M+H]<sup>+</sup>), 351.86 ([M+Na]<sup>+</sup>) and HR-ESI-MS for C<sub>20</sub>H<sub>14</sub>FN<sub>4</sub> ([M+H]<sup>+</sup>) Calcd: 329.1197; Found: 329.1195.

#### Synthesis of <sup>4</sup>F<sub>2</sub>-FBimbe 8

A solution of 5-fluoro-benzene-1,3-dicarbaldehyde (53 mg, 0.35 mmol) and 3-fluoro-1,2-benzenediamine (91 mg, 0.72 mmol) in CH<sub>3</sub>CN (3 mL) was refluxed. The reaction was monitored with TLC (CHCl<sub>3</sub>/CH<sub>3</sub>OH, 20/1, v/v). After 48 h, the reaction solution was concentrated under reduced pressure. The obtained residue was purified with chromatography on a silica gel column, eluted with a mixture of CHCl<sub>3</sub>/CH<sub>3</sub>OH (125/1, v/v) to give <sup>4</sup>F<sub>2</sub>-FBimbe 8 (41 mg, 32%) having mp 291.8-292.7 °C; <sup>1</sup>H NMR (DMSO-*d*<sub>6</sub>, 400 MHz) δ 9.05 (s, 1H), 8.24 (d,  $J = 9.6$  Hz, 2H), 7.74 (d,  $J = 8.0$  Hz, 2H), 7.28-7.23 (m, 2H), 7.09-7.05 (m, 2H); <sup>13</sup>C NMR (DMSO-*d*<sub>6</sub>, 100 MHz) δ 163.1 (d,  $J = 242.2$  Hz), 150.7, 150.6, 133.1 (d,  $J = 8.9$  Hz), 123.7 (d,  $J = 6.3$  Hz), 121.6, 115.1 (d,  $J = 23.9$  Hz), 107.8 (d,  $J = 16.7$  Hz); ESI-MS:  $m/z$  365.82 ([M+H]<sup>+</sup>), 387.77 ([M+Na]<sup>+</sup>) and HR-ESI-MS for C<sub>20</sub>H<sub>12</sub>F<sub>3</sub>N<sub>4</sub> ([M+H]<sup>+</sup>) Calcd: 365.1009; Found: 365.1008.

#### Synthesis of <sup>5</sup>F<sub>2</sub>-FBimbe 9

A solution of 5-fluoro-benzene-1,3-dicarbaldehyde (31 mg, 0.21 mmol) and 4-fluoro-1,2-benzenediamine (84 mg, 0.67 mmol) in DMSO (3 mL) was stirred at room temperature. The reaction was monitored with TLC (CHCl<sub>3</sub>/CH<sub>3</sub>OH, 20/1, v/v). After 48 h, the reaction solution was added to water (200 mL). The resulting precipitates were collected through filtration, and purified by chromatography on a silica gel column, eluted with a mixture of CHCl<sub>3</sub>/CH<sub>3</sub>OH (110/1, v/v) to give <sup>5</sup>F<sub>2</sub>-FBimbe 9 (27 mg, 35%) having mp 288.6-289.3 °C; <sup>1</sup>H NMR (DMSO-*d*<sub>6</sub>, 400 MHz) δ 13.53 (br, 2H), 8.89 (s, 1H), 8.06 (dd,  $J = 9.2$  and 0.8 Hz, 2H), 7.67 (br, 2H), 7.46 (br, 2H), 7.14 (dd,  $J = 10.0$  and 2.0 Hz, 2H); <sup>13</sup>C NMR (DMSO-*d*<sub>6</sub>, 100 MHz) δ 163.1 (d,  $J = 242.1$  Hz), 159.3 (d,  $J = 234.5$  Hz), 151.3, 149.9 (d,  $J = 3.2$  Hz), 133.3 (d,  $J = 8.9$  Hz), 123.1, 121.2, 114.5 (d,  $J = 23.8$  Hz), 111.3 (d,  $J = 25.0$  Hz); ESI-MS:  $m/z$  365.56 ([M+H]<sup>+</sup>), 387.49 ([M+Na]<sup>+</sup>) and HR-ESI-MS for C<sub>20</sub>H<sub>12</sub>F<sub>3</sub>N<sub>4</sub> ([M+H]<sup>+</sup>) Calcd: 365.1009; Found: 365.1005.

#### Synthesis of <sup>4,5</sup>F<sub>4</sub>-FBimbe 10

A solution of 5-fluoro-benzene-1,3-dicarbaldehyde (50 mg, 0.33 mmol) and 3,4-difluoro-1,2-benzenediamine (104 mg, 0.72 mmol) in DMSO (2 mL) was heated at 40 °C. The reaction was monitored with TLC (CHCl<sub>3</sub>/CH<sub>3</sub>OH, 20/1, v/v). After 24 h, the reaction mixture was added to water (200 mL) and extracted with EtOAc (100 mL×3). The organic layer was concentrated under reduced pressure to give <sup>4,5</sup>F<sub>4</sub>-FBimbe 10 (32 mg, 24%) having mp > 300 °C; <sup>1</sup>H NMR (DMSO-*d*<sub>6</sub>, 400 MHz) δ 13.61 (br, 2H), 8.86 (s, 1H), 8.06 (d,  $J = 9.6$  Hz, 2H), 7.39 (br, 2H), 7.26-7.33 (m, 2H); <sup>13</sup>C NMR (100 MHz, DMSO-*d*<sub>6</sub>) δ 162.9 (d,  $J = 242.4$  Hz), 151.8, 145.9 (d,  $J = 227.3$  Hz), 145.8 (d,  $J = 228.3$  Hz), 134.1, 133.4, 132.7 (d,  $J = 8.8$  Hz), 121.5, 115.2 (d,  $J = 23.8$  Hz), 107.9; ESI-MS:  $m/z$  401.53 ([M+H]<sup>+</sup>), 423.54 ([M+Na]<sup>+</sup>) and

HR-ESI-MS for  $C_{20}H_{10}F_5N_4$  ( $[M+H]^+$ ) Calcd: 401.0820; Found: 401.0817.

#### Synthesis of $^{4,6}F_4$ -FBimbe **11**

A solution of 5-fluoro-benzene-1,3-dicarbaldehyde (53 mg, 0.35 mmol) and 3,5-difluoro-1,2-benzenediamine (150 mg, 1.04 mmol) in DMSO (10 mL) was stirred at room temperature. The reaction was monitored with TLC ( $CHCl_3/CH_3OH$ , 20/1, v/v). After 48 h, the reaction mixture was added to water (200 mL). The resulting precipitates were collected through filtration. The precipitates were partitioned in methanol, filtered and washed with methanol to afford  $^{4,6}F_4$ -FBimbe **11** (59 mg, 42%) having mp > 300 °C;  $^1H$  NMR (DMSO- $d_6$ , 400 MHz)  $\delta$  13.64 (br, 2H), 8.86 (s, 1H), 8.07 (d,  $J = 9.6$  Hz, 2H), 7.28 (d,  $J = 7.2$  Hz, 2H), 7.14–7.08 (m, 2H);  $^{13}C$  NMR (DMSO- $d_6$ , 100 MHz)  $\delta$  162.9 (d,  $J = 242.5$  Hz), 158.8 (d,  $J = 235.4$  Hz), 158.7 (d,  $J = 235.4$  Hz), 151.2, 132.8 (d,  $J = 8.8$  Hz), 121.4, 115.0 (d,  $J = 24.0$  Hz), 98.5, 98.0; ESI-MS:  $m/z$  401.53 ( $[M+H]^+$ ) and HR-ESI-MS for  $C_{20}H_{10}F_5N_4$  ( $[M+H]^+$ ) Calcd: 401.0820; Found: 401.0815.

#### Synthesis of $^{5,6}F_4$ -FBimbe **12**

A solution of 5-fluoro-benzene-1,3-dicarbaldehyde (53 mg, 0.35 mmol) and 4,5-difluoro-1,2-benzenediamine (105 mg, 0.73 mmol) in DMSO (3 mL) was heated at 85 °C. The reaction was monitored with TLC ( $CHCl_3/CH_3OH$ , 20/1, v/v). After 48 h, the reaction solution was added to water (200 mL). The resulting precipitates were collected through filtration, and washed with methanol thrice to give  $^{5,6}F_4$ -FBimbe **12** (49 mg, 35%) having mp > 300 °C;  $^1H$  NMR (DMSO- $d_6$ , 400 MHz)  $\delta$  13.38 (br, 2H), 8.79 (s, 1H), 7.98 (d,  $J = 9.2$  Hz, 2H), 7.65 (br, 4H);  $^{13}C$  NMR (DMSO- $d_6$ , 100 MHz)  $\delta$  163.0 (d,  $J = 242.1$  Hz), 151.74, 151.73, 146.65 (dd,  $J = 238.8$  Hz and 22.6 Hz), 139.5, 132.9 (d,  $J = 8.9$  Hz), 121.0, 114.5 (d,  $J = 24.0$  Hz), 107.0, 106.3, 100.4, 99.8; negative ESI-MS:  $m/z$  399.51 ( $[M-H]^-$ ) and negative HR-ESI-MS for  $C_{20}H_8F_5N_4$  ( $[M-H]^-$ ) Calcd: 399.0675; Found: 399.0678.

#### Synthesis of $^{4,5,6,7}F_8$ -FBimbe **13**

A solution of 3,4,5,6-tetrafluorobenzene-1,2-diamine (98 mg, 0.54 mmol) and 5-fluoro-1,3-benzenedialdehyde (42 mg, 0.27 mmol) in DMSO (3 mL) was heated at 50 °C for 48 h. Then the reaction mixture was added to water (200 mL). The formed precipitates were collected through filtration and washed thoroughly with methanol to give  $^{4,5,6,7}F_8$ -FBimbe **13** (74 mg, 58%) having mp 267.0–267.8 °C;  $^1H$  NMR (DMSO- $d_6$ , 400 MHz)  $\delta$  8.81 (s, 1H), 8.05 (d,  $J = 9.2$  Hz, 2H);  $^1H$  NMR (TFA- $d$ , 400 MHz)  $\delta$  9.07 (s, 1H), 8.32 (d,  $J = 7.6$  Hz, 2H);  $^{13}C$  NMR (TFA- $d$ , 100 MHz)  $\delta$  166.1 (d,  $J = 240.8$  Hz), 151.4, 143.6 (dddd,  $J = 256.7$ , 17.2, 15.6 and 4.2 Hz), 137.7 (ddd,  $J = 255.3$ , 15.6 and 4.2 Hz), 127.6 (d,  $J = 8.5$  Hz), 126.7 ( $\times 2$ ), 123.8 (d,  $J = 25.2$  Hz), 120.0 (ddd,  $J = 16.8$ , 5.1 and 2.2 Hz); negative ESI-MS:  $m/z$  471.37 ( $[M-H]^-$ ) and HR-ESI-MS for  $C_{20}H_6N_4F_9$  ( $[M+H]^+$ ) Calcd: 473.04433; Found: 473.04366.

#### Measurement of anion recognition, anion transport and biological activity

Literature protocols were used to carry out the experiments for anion recognition,<sup>29,31</sup> vesicle formation,<sup>46</sup> pH discharge,<sup>33</sup> chloride efflux,<sup>36</sup> U-tube assay,<sup>23</sup> calcein leakage,<sup>37</sup> acridine orange staining,<sup>14–19,29,41</sup> MQAE assay,<sup>14–19,29</sup> Hoechst 33342 staining,<sup>16,17</sup> JC-1 staining<sup>16,17</sup> and MTT-based cytotoxicity assay.<sup>16,17</sup>

#### Conflicts of interest

There are no conflicts to declare.

#### Acknowledgements

This work was financially supported by the National Natural Science Foundation of China (No. 21877057).

#### Notes and references

- 1 F. Lang, M. Ritter, N. Gamper, S. Huber, S. Fillon, V. Tanneur, A. Lepple-Wienhues, I. Szabo and E. Gulbins, *Cell. Physiol. Biochem.*, 2000, **10**, 417–428.
- 2 I. Alfonso and R. Quesada, *Chem. Sci.*, 2013, **4**, 3009–3019.
- 3 P. A. Gale, J. T. Davis and R. Quesada, *Chem. Soc. Rev.*, 2017, **46**, 2497–2519.
- 4 N. Busschaert, C. Caltagirone, W. Van Rossom and P. A. Gale, *Chem. Rev.*, 2015, **115**, 8038–8155.
- 5 Z. Li and W.-H. Chen, *Mini-Rev. Med. Chem.*, 2017, **17**, 1398–1405.
- 6 D. S. Kim and J. L. Sessler, *Chem. Soc. Rev.*, 2015, **44**, 532–546.
- 7 N. Busschaert and A. P. Gale, *Angew. Chem. Int. Ed.*, 2013, **52**, 1374–1382.
- 8 G. W. Gokel and S. Negin, *Acc. Chem. Res.*, 2013, **46**, 2824–2833.
- 9 P. A. Gale, R. Pérez-Tomás and R. Quesada, *Acc. Chem. Res.*, 2013, **46**, 2801–2813.
- 10 F. De Riccardis, I. Izzo, D. Montesarchio and P. Tecilla, *Acc. Chem. Res.*, 2013, **46**, 2781–2790.
- 11 C. J. E. Haynes and P. A. Gale, *Chem. Commun.*, 2011, **47**, 8203–8209.
- 12 J. L. Sessler, L. R. Eller, W.-S. Cho, S. Nicolaou, A. Aguilar, J. T. Lee, V. M. Lynch and D. J. Magda, *Angew. Chem. Int. Ed.*, 2005, **44**, 5989–5992.
- 13 A. M. Rodilla, L. Korrodi-Gregorio, E. Hernando, P. Manuel-Manresa, R. Quesada, R. Pérez-Tomás and V. Soto-Cerrato, *Biochem. Pharm.*, 2017, **126**, 23–33.
- 14 E. Hernando, V. Soto-Cerrato, S. Cortes-Arroyo, R. Pérez-Tomás and R. Quesada, *Org. Biomol. Chem.*, 2014, **12**, 1771–1778.
- 15 V. Soto-Cerrato, P. Manuel-Manresa, E. Hernando, S. Calabuig-Farinas, A. Martinez-Romero, V. Fernandez-Duenas, K. Sahlholm, T. Knopfel, M. Garcia-Valverde, A. M. Rodilla, E. Jantus-Lewintre, R. Farras, F. Ciruela, R. Pérez-Tomás and R. Quesada, *J. Am. Chem. Soc.*, 2015, **137**, 15892–15898.
- 16 N. Busschaert, M. Wenzel, M. E. Light, P. Iglesias-Hernandez, R. Pérez-Tomás and P. A. Gale, *J. Am. Chem. Soc.*, 2011, **133**, 14136–14148.
- 17 P. I. Hernandez, D. Moreno, A. A. Javier, T. Torroba, R. Pérez-Tomás and R. Quesada, *Chem. Commun.*, 2012, **48**, 1556–1558.
- 18 T. Saha, A. Gautam, A. Mukherjee, M. Lahiri and P. Talukdar, *J. Am. Chem. Soc.*, 2016, **138**, 16443–16451.
- 19 T. Saha, M. S. Hossain, D. Saha, M. Lahiri and P. Talukdar, *J. Am. Chem. Soc.*, 2016, **138**, 7558–7567.
- 20 S. K. Ko, S. K. Kim, A. Share, V. M. Lynch, J. Park, W. Namkung, W. V. Rossom, N. Busschaert, P. A. Gale, J. L. Sessler and I. Shin, *Nat. Chem.*, 2014, **6**, 885–892.
- 21 S. Purser, P. R. Moore, S. Swallow and V. Gouverneur, *Chem. Soc. Rev.*, 2008, **37**, 320–330.

- 22 S. Bahmanjah, N. Zhang and J. T. Davis, *Chem. Commun.*, 2012, **48**, 4432–4434.
- 23 S. J. Moore, M. Wenzel, M. E. Light, R. Morley, S. J. Bradberry, P. Gomez-Iglesias, V. Soto-Cerrato, R. Pérez-Tomás and P. A. Gale, *Chem. Sci.*, 2012, **3**, 2501–2509.
- 24 L. E. Karagiannidis, C. J. E. Haynes, K. J. Holder, I. L. Kirby, S. J. Moore, N. J. Wells and P. A. Gale, *Chem. Commun.*, 2014, **50**, 12050–12053.
- 25 P. A. Gale, C. C. Tong, C. J. E. Haynes, O. Adeosun, D. E. Gross, E. Karnas, E. M. Sedenberg, R. Quesada and J. L. Sessler, *J. Am. Chem. Soc.*, 2010, **132**, 3240–3241.
- 26 N. Busschaert, S.-H. Park, K.-H. Baek, Y. P. Choi, J. Park, E. N. W. Howe, J. R. Hiscock, L. E. Karagiannidis, I. Marques, V. Felix, W. Namkung, J. L. Sessler, P. A. Gale and I. Shin, *Nat. Chem.*, 2017, **9**, 667–675.
- 27 C.-C. Peng, Z. Li, L.-Q. Deng, Z.-F. Ke and W.-H. Chen, *Bioorg. Med. Chem. Lett.*, 2016, **26**, 2442–2445.
- 28 C.-C. Peng, M.-J. Zhang, X.-X. Sun, X.-J. Cai, Y. Chen and W.-H. Chen, *Org. Biomol. Chem.*, 2016, **14**, 8232–8236.
- 29 X.-H. Yu, C.-C. Peng, X.-X. Sun and W.-H. Chen, *Eur. J. Med. Chem.*, 2018, **152**, 115–125.
- 30 C. A. Lipinski, F. Lombardo, B. W. Dominy and P. J. Feeney, *Adv. Drug Deliver. Rev.*, 1997, **23**, 3–25.
- 31 C. Montoya, R. Cervantes and J. Tiburcio, *Tetrahedron Lett.*, 2015, **56**, 6177–6182.
- 32 W. Sander and M. Exner, *J. Chem. Soc., Perkin Trans. 2*, 1999, 2285–2290.
- 33 Z. Li, X.-H. Yu, Y. Chen, D.-Q. Yuan and W.-H. Chen, *J. Org. Chem.*, 2017, **82**, 13368–13375.
- 34 S. Bhosale and S. Matile, *Chirality*, 2006, **18**, 849–856.
- 35 N. Busschaert, L. E. Karagiannidis, M. Wenzel, C. J. E. Haynes, N. J. Wells, P. G. Young, D. Makuc, J. Plavec, K. A. Jolliffe and P. A. Gale, *Chem. Sci.*, 2014, **5**, 1118–1127.
- 36 J. T. Davis, P. A. Gale, O. A. Okunola, P. Prados, J. C. Iglesias-Sanchez, T. Torroba and R. Quesada, *Nat. Chem.*, 2009, **1**, 138–144.
- 37 Y. Yang, X. Wu, N. Busschaert, H. Furuta and P. A. Gale, *Chem. Commun.*, 2017, **53**, 9230–9233.
- 38 L. A. Jowett, E. N. W. Howe, V. Soto-Cerrato, W. Van Rossom, R. Pérez-Tomás and P. A. Gale, *Sci. Rep.*, 2017, **7**, 9397.
- 39 I. Izzo, S. Licen, N. Maulucci, G. Autore, S. Marzocco, P. Tecilla and F. De Riccardis, *Chem. Commun.*, 2008, 2986–2988.
- 40 M. Olivari, R. Montis, L. E. Karagiannidis, P. N. Horton, L. K. Mapp, S. J. Coles, M. E. Light, P. A. Gale and C. Caltagirone, *Dalton Trans.*, 2015, **44**, 2138–2149.
- 41 X.-Q. Hong, X.-H. Yu, K. Zhang and W.-H. Chen, *Org. Biomol. Chem.*, 2018, **16**, 8025–8029.
- 42 M. Tsukimoto, H. Harada, A. Ikari and K. Takagi, *J. Biol. Chem.*, 2005, **280**, 2653–2658.
- 43 C. D. Bortner and J. A. Cidlowski, *J. Biol. Chem.*, 2003, **278**, 39176–39184.
- 44 L. Galluzzi, I. Vitale, J. M. Abrams, E. S. Alnemri, E. H. Baehrecke, M. V. Blagosklonny, T. M. Dawson, V. L. Dawson, W. S. El-Deiry, S. Fulda, E. Gottlieb, D. R. Green, M. O. Hengartner, O. Kepp, R. A. Knight, S. Kumar, S. A. Lipton, X. Lu, F. Madeo, W. Malorni, P. Mehlen, G. Nunez, M. E. Peter, M. Piacentini, D. C. Rubinsztein, Y. Shi, H. U. Simon, P. Vandenabeele, E. White, J. Yuan, B. Zhivotovsky, G. Melino and G. Kroemer, *Cell Death Differ.*, 2011, **19**, 107–120.
- 45 A. Perelman, C. Wachtel, M. Cohen, S. Haupt, H. Shapiro and A. Tzur, *Cell Death Dis.*, 2012, **3**, e430.
- 46 W.-H. Chen and S. L. Regen, *J. Am. Chem. Soc.*, 2005, **127**, 6538–6539.